SAND2019-14612C

Multi-Stage Stabilized Continuation for Indirect Optimal Control of Hypersonic Trajectories

Mihir Vedantam* and Maruthi R. Akella†
The University of Texas at Austin, Austin, Texas, 78712, United States

Michael J. Grant‡
Sandia National Labs, Albuquerque, New Mexico, 87123, United States

This work presents the application of stabilized continuation to the planar unpowered hypersonic trajectory generation problem using indirect optimal control methods. This scheme is non-iterative and guaranteed to terminate within a finite number of floating point operations - thereby making it well-suited for onboard autonomous operations. This algorithm involves using the stabilized continuation method in multiple stages starting with a "loose" integration tolerance and subsequently ramping up toward a "strict" integration tolerance. An important outcome of this approach is that even when the underlying optimal control problem governing the planar hypersonic trajectory becomes numerically stiff, our studies indicate that the stabilized continuation scheme terminates successfully with a converged solution.

I. Introduction

Optimal trajectory generation is a computationally difficult problem for hypersonic applications due to the nonlinearity in the governing dynamics and sensitive dependence upon atmospheric density variations with altitude. The computational complexity associated with trajectory generation is particularly formidable during the unpowered parts of the flight regime that involve atmospheric reentry. The major contribution of this paper is the development of a multi-stage stabilized continuation scheme that is customized for hypersonic trajectory generation applications using indirect optimal control techniques.

Traditionally, optimal trajectories for hypersonic applications are generated offline using direct methods or evolutionary methods due to the relative ease with which they can be implemented, aided by the availability of many commercial software tools [1, 2]. Early efforts in this field mostly focused on using pseudo-spectral methods [3–5] and collocation methods [6, 7]. Recent implementations of direct optimal control approaches involve using powerful search algorithms such as the fireworks algorithm [8] or particle swarm optimization [9] to search over a large control vector space for an optimal solution. The fireworks algorithm involves seeding several "fireworks" over the search space and the promising fireworks are "exploded" into sparks to search the surrounding areas. The particle swarm method seeds several particles in the search space and uses techniques like gradient descent to find optimal solutions. One key feature of both of these prior works is that they present algorithms to automatically tune the parameters of the search process, thereby helping automate the search algorithm. However, neither of these approaches are able to rigorously guarantee convergence to an optimal solution.

On the other hand, the application of indirect methods for hypersonic trajectory guidance has been generally avoided despite their accuracy and provable optimality properties due to numerical difficulties associated with the onboard implementation of shooting methods. However, Grant et al. [10–12] demonstrated the possibilities for solving indirect hypersonic trajectory optimization problems with high accuracy. By employing symbolic math engines such as SymPy or MATLAB's Symbolic Toolbox, a framework for the automated generation of the necessary conditions of optimality was developed. The resulting optimal control problem is shown to be well-suited for the application of continuation methods. More recently, these indirect approaches have been expanded to reformulate multi-point boundary value problems resulting from inequality constraints into two-point boundary value problems through the introduction of sigmoid functions [13]. However, one limitation of this method is that the continuation scheme has to be predetermined.

*Graduate Research Assistant, Aerospace Engineering and Engineering Mechanics, 2617 Wichita St, Austin, TX 78712; AIAA Student Member.
†E.P. Schoch Professor, Aerospace Engineering and Engineering Mechanics, 2617 Wichita Street, Austin, TX 78712; AIAA Associate Fellow
‡Principal Aeronautical Engineer, Aerospace Systems Analysis, Sandia National Laboratories, New Mexico, P.O. Box 5800, Albuquerque, NM 87185-1162; AIAA Senior Member.

Since continuation methods present themselves as effective candidates toward solving the indirect optimal hypersonic trajectory generation problem, a natural progression is to consider the application of stabilized continuation techniques [14]. In [15], a unified framework for applying stabilized continuation to both finite and infinite dimensional systems is presented, showcasing the method's effectiveness.

In this work, we take the prior work completed in [15] and apply it to the family of hypersonic problems by expanding to a multi-staged stabilized continuation scheme. We present the application of a multi-stage stabilized continuation method to the planar hypersonic optimal control trajectory generation problem. The multi-stage approach involves using the stabilized continuation method in multiple stages with increasingly strict tolerances. The remainder of this paper is organized as follows: Section II presents an overview of the stabilized continuation algorithm along with the derivation of the planar hypersonic optimal control trajectory generation problem. Section III presents the application of the stabilized continuation algorithm to the planar hypersonic optimal control trajectory generation problem along with numerical studies used to tune the algorithm. Lastly, Section IV presents the multi-staged stabilized continuation approach along with the discovery of bifurcation points in the initial guess space.

II. Background

A. Overview of Stabilized Continuation

Stabilized continuation offers three major advantages over traditional continuation, making stabilized continuation a particularly powerful boundary value problem solver: (1) It provides for adaptive step-size selection. (2) It guarantees the terminal condition error attenuates over the continuation interval in a numerically stable fashion. (3) The stabilizing term can be selected such that the terminal condition error is reduced to zero over the user-specified continuation interval. These three features are highlighted in the following derivation of stabilized continuation.

Continuation schemes are usually applied toward solving a system of nonlinear equations of the following form,

$$F(z(s), s) = 0 \tag{1}$$

wherein z is the vector of all unknown variables associated with the two-point boundary value problem (TPBVP). In the case of indirect optimal control problems, these unknown variables are typically the unconstrained state and co-state initial conditions, and the time-of-flight in the case of free final-time problems. The function $F(z, s)$ represents the boundary conditions, and the continuation parameter, s, acts to parameterize the system of nonlinear equations in Eq. 1 such that over the interval $s \in [s_0, s_f]$, a known solution is transformed into a desired solution.

For classical implementations of the continuation algorithm, the forward progression of the continuation parameter is typically user specified. However, with the application of the Davidenko equation (2), traditional continuation can be transformed into an ordinary differential equation (ODE):

$$\frac{\mathrm{d}}{\mathrm{d}s}F(z, s) = 0 = \frac{\partial F}{\partial z}\frac{\mathrm{d}z}{\mathrm{d}s} + \frac{\partial F}{\partial s} \tag{2}$$

Which can then be re-arranged as,

$$\frac{\mathrm{d}z}{\mathrm{d}s} = -\frac{\partial F}{\partial z}^{-1}\frac{\partial F}{\partial s} \tag{3}$$

This transformation recasts the original TPBVP into an initial value problem (IVP) which (1) allows the usage of variable step-size integrators such as MATLAB's *ode45*, and (2) removes the need for the user to pick the step-size for the forward evolution of the continuation parameter s.

However, Eq. 3 provides no additional mechanisms to attenuate the error over the continuation interval. If a bad initial guess is given to the continuation scheme ($F(z, 0) \neq 0$), the terminal solution will also generally result in poor outcomes, or potentially, even convergence failure. To ensure that error does not accumulate or propagate through the continuation interval, Eq. 2 can be augmented with a "stabilizing term" in the following manner,

$$\frac{\partial F}{\partial z}\frac{\mathrm{d}z}{\mathrm{d}s} + \frac{\partial F}{\partial s} = A_m F(z, s) + \nu_s \tag{4}$$

Which can be rearranged as,

$$\frac{\mathrm{d}z}{\mathrm{d}s} = \left[\frac{\partial F}{\partial z}\right]^{-1}\left[A_m F(z, s) + \nu_s - \frac{\partial F}{\partial s}\right],\ s \in [s_0, s_f],\ z(s_0) \text{ given} \tag{5}$$

The term $A_m F(z, s)$ acts as a stabilizing linear feedback for the boundary condition error when A_m is selected to be any Hurwitz matrix. Finally, if the stabilizing term, ν_s, is selected to be the linear time invariant (LTI) system minimum effort control law,

$$\nu_s = -\Phi_m(s_0, s) W_c^{-1} \Phi_m(s_0, s) \tag{6}$$

the continuation algorithm is guaranteed to regulate the error variables $F(z, s)$ to zero over one continuation interval. The term W_c is the controllability Grammian matrix and $\Phi(s_0, s)$ is the state transition matrix of the LTI system:

$$W_c(s_1, s_2) = \int_{s_1}^{s_2} \Phi_m(s_1, \eta) \Phi_m^T(s_1, \eta) d\eta \tag{7}$$

$$\Phi_m(s_0, s) = e^{A_m(s - s_0)} \tag{8}$$

B. Planar Hypersonic Optimal Trajectory Generation Problem

In this work, the planar hypersonic optimal trajectory generation problem is considered. The equations of motion of an unpowered hypersonic vehicle in planar motion are as follows:

$$\begin{aligned} \dot{h} &= v \sin\gamma \\ \dot{\theta} &= \frac{v \cos\gamma}{r} \\ \dot{v} &= \frac{-D}{m} - \frac{\mu \sin\gamma}{r^2} \\ \dot{\gamma} &= \frac{L}{mv} + \left(\frac{v}{r} - \frac{\mu}{vr^2}\right) \cos\gamma \end{aligned} \tag{9}$$

In Eq. 9, h represents the altitude of the vehicle, θ is the longitude, v is the velocity, and γ is the flight path angle. The control input, angle of attack (α), appears explicitly in the lift and drag terms which are computed as:

$$\begin{aligned} C_D &= 1.6537\alpha^2 + 0.0612 \\ C_L &= 1.5658\alpha \\ D &= \frac{1}{2}\rho v^2 C_D A_{ref} \\ L &= \frac{1}{2}\rho v^2 C_L A_{ref} \end{aligned} \tag{10}$$

The density of the atmosphere is drawn from an exponential model:

$$\rho = \rho_0 \exp\left(-\frac{h}{H}\right) \tag{11}$$

The radial distance for a spherical Earth, r, measured in terms of the radius of both Earth's radius r_e and altitude h is given by:

$$r = r_e + h \tag{12}$$

The remaining terms in Eqns. 9, 10, 11 and 12 are environmental and vehicle parameters. The values selected for these parameters in this study are documented in Table 1.

Parameter	Symbol	Value
Surface air density	ρ_0	1.2 kg/m^3
Vehicle reference area	A_{ref}	0.2919 m^2
Gravitational constant	μ	$3.986 * 10^{-14}$ m^3/s^2
Mass	m	340.1943 kg
Scale height	H	7500 m
Radius of Earth	r_e	6378000 m

Table 1 Vehicle and environment parameters.

The maximum velocity upon impact cost is considered as the optimality criterion, J, for this paper. This can be represented as,

$$J = -v(t_f)^2 \tag{13}$$

Thus, the goal is to minimize this cost functional while satisfying some constraints on the states. An example set of initial and terminal state constraints can be found in Table 2.

Variable	Deployment ($t = 0$)	Impact ($t = t_f$)
Time, t	$t_0 = 0$	free t_f
Altitude, h	80,000 m	0 m
Velocity Magnitude, v	4,000 m/s	free
Flight-path Angle, γ	free	free
Longitude, θ	0°	5°

Table 2 Initial and terminal constraints.

The constraints and cost functional serve as the basis for the indirect optimal control formulation. To transform this into a TPBVP, the Euler-Lagrange necessary optimality conditions can be applied as follows:

$$\mathcal{H} = \mathcal{L} + \lambda^T f + \mu^T c \tag{14}$$

$$\dot{\lambda} = -\left(\frac{\partial \mathcal{H}}{\partial x}\right)^T \tag{15}$$

$$\lambda(t_f) = \left(\frac{\partial \phi}{\partial x}\right)^T \Big|_t \tag{16}$$

$$0 = \left(\frac{\partial \mathcal{H}}{\partial u}\right)^T \tag{17}$$

In Eq. 14, $\mathcal{H}$ represents the Hamiltonian of the system, $\mathcal{L}$ represents the Lagrangian (i.e., the integrand of the cost functional), λ is the vector of Lagrange multipliers used to adjoin the equations of motion (f) and μ is the vector of Lagrange multipliers used to adjoin the additional path constraints, c. In Eq. 15, x represents the vector of states, i.e., $x = [h\ v\ \theta\ \gamma]^T$. In Eq. 16, ϕ represents the non integrated part of the cost functional with the initial and terminal state constraints adjoined. In Eq. 17, u represents the vector of control inputs. Since there is no Lagrange cost and no path constraints, the Hamiltonian of the system is simply the co-states multiplied by the state rates,

$$\mathcal{H} = \lambda_h \dot{h} + \lambda_\theta \dot{\theta} + \lambda_v \dot{v} + \lambda_\gamma \dot{\gamma} \tag{18}$$

Then, Eq. 15 can be applied to find the rate-of-change of the Lagrange multipliers corresponding to each state (referred to as co-states). The explicit representations of the co-state rates are omitted for conciseness, but can be computed as follows,

$$\begin{aligned}\dot{\lambda_h} &= -\frac{\partial \mathcal{H}}{\partial h} \\ \dot{\lambda_\theta} &= -\frac{\partial \mathcal{H}}{\partial \theta} \\ \dot{\lambda_v} &= -\frac{\partial \mathcal{H}}{\partial v} \\ \dot{\lambda_\gamma} &= -\frac{\partial \mathcal{H}}{\partial \gamma}\end{aligned} \tag{19}$$

For the planar hypersonic optimal trajectory problem to be a well posed TPBVP, a total of ten boundary conditions are required; however, Table 2 only provides six, since four of the conditions are free. For the additional constraints, Eq. 16 can be applied at $t = t_f$ and $t = t_0$ to find boundary conditions for the co-states at deployment and impact, respectively. The application of Eq. 16 results in the remaining four boundary conditions:

$$\begin{aligned}\lambda_\gamma(0) &= 0 \\ \lambda_\gamma(t_f) &= 0 \\ \lambda_v + 2v &= 0 \\ \mathcal{H}(t_f) &= 0\end{aligned} \tag{20}$$

Finally, the dependency of the equations of motion on the control vector must be removed for the problem to truly be a TPBVP. To accomplish this task, Eq. 17 can be used to represent the angle-of-attack in terms of the states and co-states:

$$\alpha = 0.4734\frac{\lambda_\gamma}{\lambda_v v} \tag{21}$$

Whenever the control term, α, appears in the equations-of-motion and the co-state rates, it will be replaced by Eq. 21. The optimal control problem is now represented as a TPBVP with the state vector consisting of the original states and the co-states and the boundary conditions being a combination of the boundary conditions on the original states and the co-state boundary conditions. Since the optimal control problem is now recast into a TPBVP, the stabilized continuation algorithm (Eq. 5) can now be used to solve it.

III. Application of Stabilized Continuation to the Planar Hypersonic Problem

The terminal boundary conditions shown in Table 2 and Eq. 20 can be collected together to form the nonlinear system of equations in the stabilized continuation formulation:

$$F(z(s), s) = \begin{bmatrix} h(t_f) - h_f \\ \theta(t_f) - \theta_f \\ \lambda_v + 2v(t_f) \\ \lambda_\gamma(t_f) \\ \mathcal{H}(t_f) \end{bmatrix} = 0 \tag{22}$$

In Eq. 22, $z(s)$ represents the vector of unknown states and co-states at $t = t_0$:

$$z(s) = [\lambda_h \ \lambda_\theta \ \lambda_v \ \gamma \ t_f]^T \tag{23}$$

Similarly, the vector of states can be collected as:

$$x(s) = [h\ \theta\ v\ \gamma\ \lambda_h\ \lambda_\theta\ \lambda_v\ \lambda_\gamma\ t_f]^T \tag{24}$$

Because the stabilized continuation algorithm will be implemented numerically, it is critical to scale the variables such that the Jacobian matrix of the state and co-state rates is well conditioned. The scale factors used in this work are from [16]:

$$\begin{aligned} h_{scale} &= r_e \\ t_{scale} &= \sqrt{r_e/g_0} \\ v_{scale} &= \sqrt{r_e g_0} \end{aligned} \tag{25}$$

For the purposes of this work, the feedback matrix, A_m, is simplified into an identity matrix multiplied by a negative scalar constant (i.e., βI). However, it is possible to select feedback matrices that exploit any relevant structure in the problem. One simple example would be to select a diagonal matrix with different feedback gains for each element of the z vector. The term $\frac{\partial F}{\partial z}$ represents the sensitivity of the terminal boundary conditions to the guess vector, z. To compute this matrix, the following representation can be used:

$$\frac{\partial F}{\partial z} = \frac{\partial F}{\partial x(t_f)} \frac{\partial x(t_f)}{\partial z} \tag{26}$$

Since the guess vector, z, is the collection of unknowns at the initial time, t_0, and the boundary conditions of concern are the terminal time conditions, the term $\frac{\partial x}{\partial z}$ contains the elements of the state transition matrix that correspond to the pair $(x,\ z)$ which can be computed with the state transition matrix differential equation:

$$\frac{\partial x}{\partial z} = \Phi(t_0, t_f) \tag{27}$$

$$\dot{\Phi}(t_0, t_f) = A(x)\Phi(t_0, t_f) \tag{28}$$

$$A(x) = \frac{\partial \dot{x}(t)}{\partial x} \tag{29}$$

Since the continuation parameter, s, does not appear explicitly in the state rate equations, it can be continued on implicitly by leaving the terminal boundary conditions in the form $F(z(s))$ or it can be explicitly embedded in the terminal boundary condition errors, $F(z(s), s)$. An example formulation of explicitly continuing on the terminal downrange over the course of the continuation interval is as follows:

$$\theta_f(s) = s\theta_{\text{desired}} + (1 - s)\theta_{\text{initial}} \tag{30}$$

The initial guess given to the stabilized continuation algorithm can be integrated forward to obtain $\theta_{initial}$, which is the terminal value of the downrange at $s = 0$. The numerical robustness properties of the stabilized continuation algorithm applied to the planar hypersonic trajectory generation optimal control problem is shown with this embedded continuation parameter in 1.

In Fig. 1, a 20km downrange trajectory is given to the stabilized continuation algorithm as an initial guess. Since generating an optimal straight down trajectory is numerically easy, it is generated by using stabilized continuation without any parameter embedding. However, it is important to note that the initial guess need not be generated by stabilized continuation: this is simply done to showcase the numerical robustness properties of stabilized continuation in an intuitive manner. Then Eq. 30 is used to morph the terminal downrange from the initial guess terminal condition (20km) to the desired terminal downrange (1450 km) over the course of the continuation interval. Lastly, Eq. 5 is integrated over $s \in [0, 1]$ because this formulation allows the initial and desired downranges to be explicitly expressed in the parameter embedding formula (Eq. 30). The integration tolerances (absolute and relative) are set to 10^{-8}, because they correlate with a one meter downrange and altitude accuracy. MATLAB's *ode45* is used to integrate Eq. 5, and

completes the integration in 41 integration steps, of which the initial and terminal steps along with three interim solutions are shown in Fig. 1.

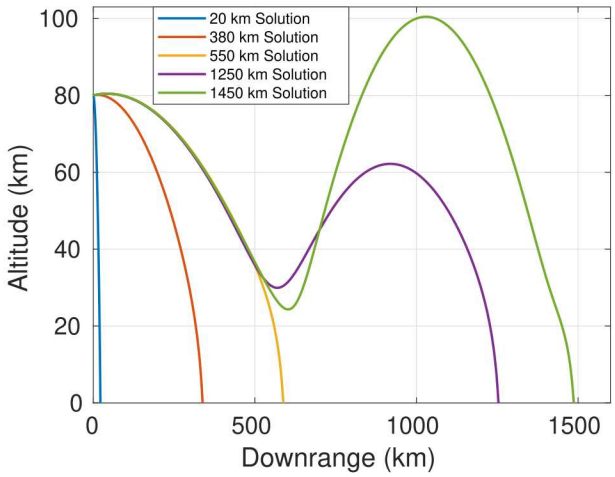

Fig. 1 Trajectory is transformed from the initial (blue) guess to the desired (green) trajectory

A. Parameter Tuning

Since stabilized continuation is seen to be a generally effective method for solving hypersonic trajectory generation problems, the next step is to address the question of how to tune the various parameters associated with the continuation algorithm (namely, A_m, and the numerical tolerances governing the implementation of the variable step-size integrator) such that the numerical integration of Eq. 5 proceeds within the least number of computational steps. For the purposes of this study, the stability matrix A_m is chosen to be $A_m = \beta I$, i.e., a negative scalar β (for algorithm simplicity). This results in three main parameters to consider when integrating the stabilized continuation ODE (Eq. 5): relative tolerance, absolute tolerance, and the value of the stability parameter β. The results of conducting a parameter tuning study with regards to the stabilized continuation algorithm are reported in Fig. 2.

In Fig. 2, the absolute and relative tolerances are set to the same value for ease-of-presentation. It is important to recognize that when the magnitude of the stability parameter $|\beta|$ is small, the stabilized algorithm is invariant to the integration tolerance setting and converges to the same solution (i.e., same terminal condition error value for $F(z(s_f), s_f)$). However, the right-hand plot in Fig. 2 showcases that the algorithm takes significantly more integration steps to converge to the same solution if the integration tolerance is made stricter. This result itself is a major contribution of this work. More specifically, instead of a single-stage continuation, a multi-stage approach for stabilized continuation can allow for significantly fewer integration steps being taken over the course of the continuation interval.

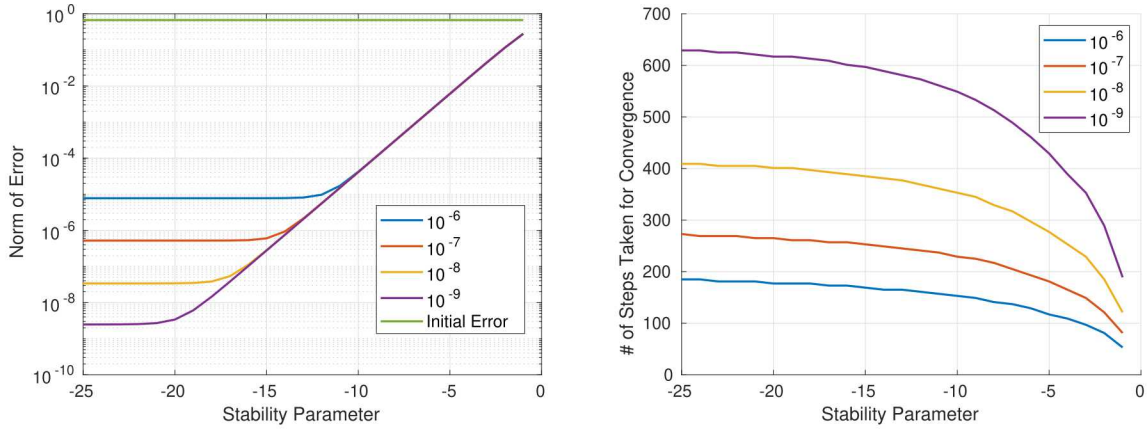

Fig. 2 Numerical studies showcasing how changes to specific parameters within the stabilized continuation algorithm impact overall numerical convergence properties

IV. Multi-Stage Stabilized Continuation

Qualitatively speaking, the multi-stage approach involves solving the optimal control problem at a "loose" integration tolerance and small $|\beta|$, then sequentially using the resulting solution to seed the subsequent stage of stabilized continuation to compute a higher quality solution that uses tighter tolerances. This way the higher computational cost for solving with a "strict" integration tolerance and large $|\beta|$ is not paid in the beginning stages of the continuation process.

A. Comparing Multi-Stage Schemes

With the range of acceptable tolerances being predetermined and only considering tolerances that are powers of 10, the maximum number of stages considered is five ($[10^{-4}, 10^{-5}, 10^{-6}, 10^{-7}, 10^{-8}]$). With these constraints, single-staged stabilized continuation can be compared with two, three, four, and five-staged stabilized continuation. In each class of multi-staged stabilized continuation, every combination of tolerances is also considered. A comparison of all the four best possible multiple stage stabilized continuation schemes is provided in Fig. 3.

In Fig. 3, the two-stage scheme takes the least number of computational steps (left-hand plot) while converging to an equal quality solution as the rest of the multi-stage schemes (right-hand plot) except for where the perfect solution is given as a guess (approximately at 550 km downrange). Also notably, the multi-stage schemes far outperform the single-stage scheme in terms of computational effort and convergence rates. The single-stage method converges to a high-quality solution in a small region around where it is already given the exact solution at the start of the continuation process whereas all of the multi-staged schemes converge to a high-quality solution even where the terminal downrange is between $\theta_{km} \approx 20\ km$ and $\theta_{km} \approx 1450\ km$. When the multi-staged approaches are unable to converge to a high-quality solution, the multi-staged approaches take significantly more computational steps than the single-staged approach. In particularly egregious cases (i.e., $\theta_{km} = 0\ km$), the two-staged approach takes almost twice as long to terminate. However, even where the multi-staged approach fails to converge, it still manages to outperform the single-staged approach in terms of the quality of the solution.

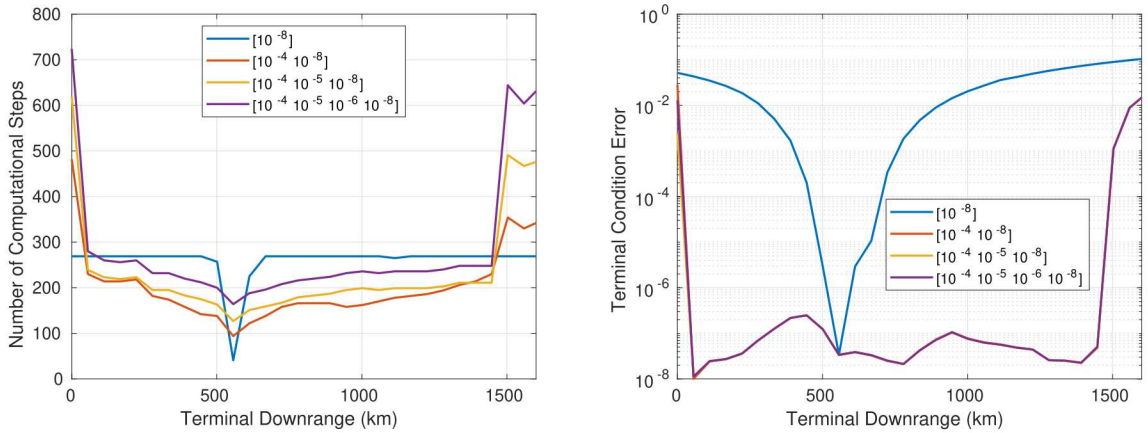

Fig. 3 Comparison of the best two-stage, three-stage, four-stage and five-stage stabilized continuation schemes.

B. Discovery of Bifurcation Points

Selecting an integration tolerance "looser" than 10^{-4} demonstrates the robustness of the multi-staged stabilized continuation algorithm despite resulting in the possibility of finite-time escapes during numerical integration. This demonstration is through the discovery of bifurcation points over the course of the trajectory, where the terminal solution transitions from one class of optimal solutions to another. This transition is shown in Fig. 4.

In Fig. 4, an optimal solution subject to the boundary conditions present in Table 2 serves as a baseline initial guess. Then the initial λ_h value is varied and given to the two-staged stabilized continuation algorithm with an initial integration tolerance of 10^{-2} and a final stage integration tolerance of 10^{-8}. This serves as a study of the two-staged stabilized continuation method's robustness to a bad initial guess, where only one of the guess values is incorrect. The left-hand plot in Fig. 4 compares the initial $\lambda_h(0)$ guess with the $\lambda_h(0)$ solution produced by the multi-staged method. It is clear that the solution for λ_h switches from $\lambda_h \approx 0$ to $\lambda_h \approx -1.7$ where the initial guess on λ_h is less than $\lambda_h \approx -0.2$. Looking at the right-hand plot in Fig. 4, the new solution is of lower quality (higher terminal condition error), but still meets the required integration tolerances specified. The most interesting aspect of this transition, however, is that the solution transitions from a *maximum energy* solution to a *minimum energy* solution. This fact is best showcased in Fig. 5.

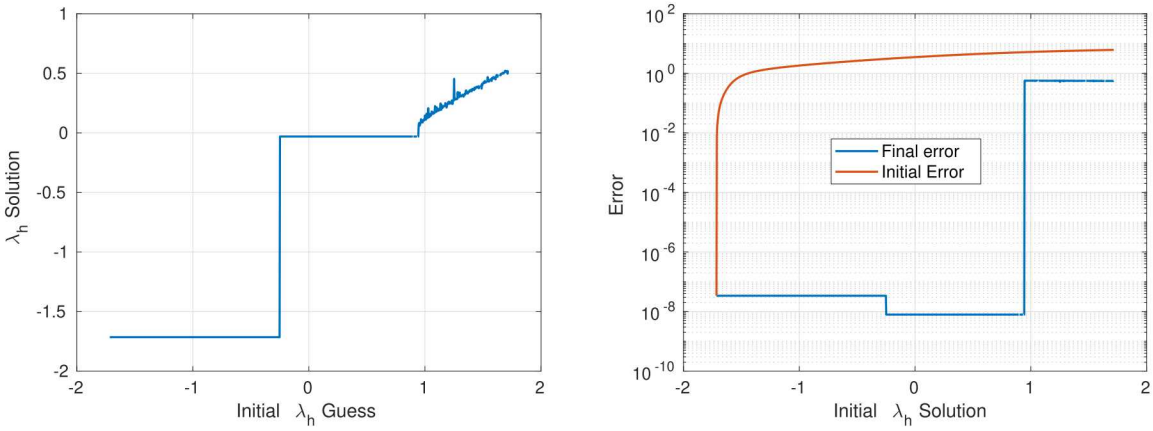

Fig. 4 Initial co-state guess' effect on final co-state solution and convergence.

In Fig. 5, the minimum energy solution and maximum energy solution are the same until approximately 145 seconds. Beyond the 145 second mark, the minimum energy solution appends an in-place dive and climb maneuver where it passes the desired terminal state and loops back up to bleed energy. One interesting detail specific to this problem is that

the minimum energy solution and maximum energy solution would be the same when implemented in a real system due to the minimum energy solution completing its dive and climb maneuver below 0 km altitude. The important feature to observe is that even where multistage stabilized continuation encounters numerical stiffness, it is still robust enough to find a high quality trajectory that satisfies the boundary conditions.

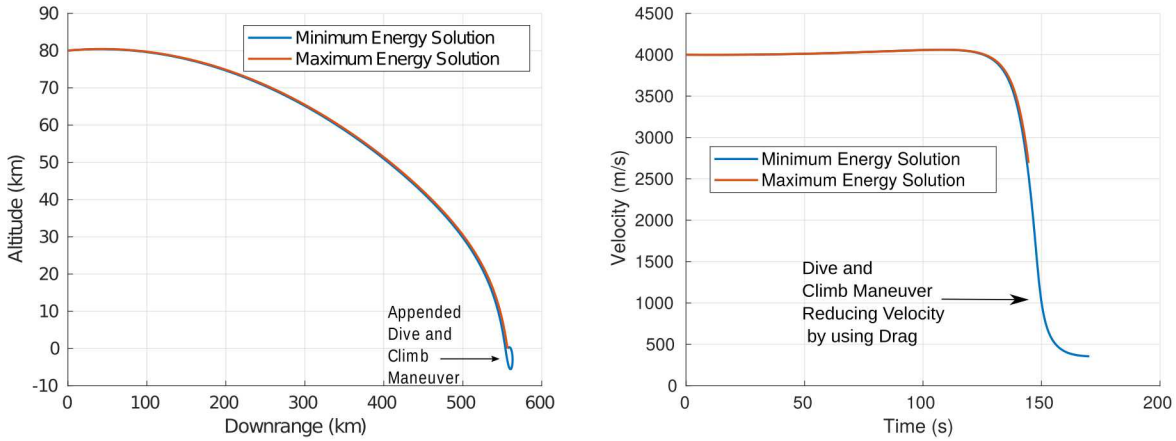

Fig. 5 Maximum energy solution versus minimum energy solution.

V. Conclusion

This work presented the application of the stabilized continuation boundary value problem solver to the unpowered hypersonic trajectory generation problem. Stabilized continuation serves as a natural progression from traditional continuation methods in conjunction with indirect methods. The numerical studies presented in this work indicate that the multistage stabilized continuation is both computationally more efficient than single-staged stabilized continuation and more robust to low-quality initial guesses. The key result is that the multi-stage stabilized continuation approach is able to find solutions even where the problem becomes numerically stiff. These solutions are a transition from maximum energy to minimum energy solutions. However, the discovery of bifurcation points and using the stabilized continuation method with the least computational burden still requires some intervention from the designer. Future work will investigate automatically tuning the multi-stage scheme as well as the stability parameter.

References

[1] Gill, P. E., Murray, W., and Saunders, M. A., "SNOPT: An SQP algorithm for large-scale constrained optimization," *SIAM Rev.*, Vol. 47, 2005, pp. 99–131.

[2] Schlueter, M., Erb, S. O., Gerdts, M., Kemble, S., and Rückmann, J.-J., "MIDACO on MINLP space applications," *Advances in Space Research*, Vol. 51, No. 7, 2013, pp. 1116–1131.

[3] Park, J.-W., Tahk, M.-J., and Sung, H.-G., "Trajectory optimization for a supersonic air-breathing missile system using pseudo-spectral method," *International Journal of Aeronautical and Space Sciences*, Vol. 10, No. 1, 2009, pp. 112–121.

[4] Fahroo, F., and Ross, I. M., "Direct trajectory optimization by a Chebyshev pseudospectral method," *Journal of Guidance, Control, and Dynamics*, Vol. 25, No. 1, 2002, pp. 160–166.

[5] Darby, C. L., Hager, W. W., and Rao, A. V., "Direct trajectory optimization using a variable low-order adaptive pseudospectral method," *Journal of Spacecraft and Rockets*, Vol. 48, No. 3, 2011, pp. 433–445.

[6] Benson, D. A., Huntington, G. T., Thorvaldsen, T. P., and Rao, A. V., "Direct trajectory optimization and costate estimation via an orthogonal collocation method," *Journal of Guidance, Control, and Dynamics*, Vol. 29, No. 6, 2006, pp. 1435–1440.

[7] Herman, A. L., and Conway, B. A., "Direct optimization using collocation based on high-order Gauss-Lobatto quadrature rules," *Journal of Guidance, Control, and Dynamics*, Vol. 19, No. 3, 1996, pp. 592–599.

[8] Wei, X., Liu, L., Wang, Y., and Yang, Y., "Reentry Trajectory Optimization for a Hypersonic Vehicle Based on an Improved Adaptive Fireworks Algorithm," *International Journal of Aerospace Engineering*, Vol. 2018, 2018.

[9] Li, Z., Hu, C., Ding, C., Liu, G., and He, B., "Stochastic gradient particle swarm optimization based entry trajectory rapid planning for hypersonic glide vehicles," *Aerospace Science and Technology*, Vol. 76, 2018, pp. 176–186.

[10] Grant, M., Clark, I., and Braun, R., "Rapid simultaneous hypersonic aerodynamic and trajectory optimization using variational methods," *AIAA Atmospheric Flight Mechanics Conference*, 2011, p. 6640.

[11] Grant, M. J., and Braun, R. D., "Rapid indirect trajectory optimization for conceptual design of hypersonic missions," *Journal of Spacecraft and Rockets*, Vol. 52, No. 1, 2014, pp. 177–182.

[12] Grant, M. J., and Antony, T., "Rapid indirect trajectory optimization of a hypothetical long range weapon system," *AIAA Atmospheric Flight Mechanics Conference*, 2016, p. 0276.

[13] Saranathan, H., and Grant, M. J., "Relaxed Autonomously Switched Hybrid System Approach to Indirect Multiphase Aerospace Trajectory Optimization," *Journal of Spacecraft and Rockets*, Vol. 55, No. 3, 2017, pp. 611–621.

[14] Ohtsuka, T., and Fujii, H., "Stabilized continuation method for solving optimal control problems," *Journal of Guidance, Control, and Dynamics*, Vol. 17, No. 5, 1994, pp. 950–957.

[15] Kotamraju, G. R., and Akella, M. R., "Stabilized continuation methods for boundary value problems," *Applied Mathematics and Computation*, Vol. 112, No. 2-3, 2000, pp. 317–332.

[16] Lu, P., "Entry guidance: a unified method," *Journal of Guidance, Control, and Dynamics*, Vol. 37, No. 3, 2014, pp. 713–728.